

Chapter 3

COMPUTER SIMULATION OF RADON MEASUREMENTS WITH NUCLEAR TRACK DETECTORS

D. Nikezic and K.N. Yu

Department of Physics and Materials Science, City University of Hong Kong,
Tat Chee Avenue, Kowloon Tong, Hong Kong

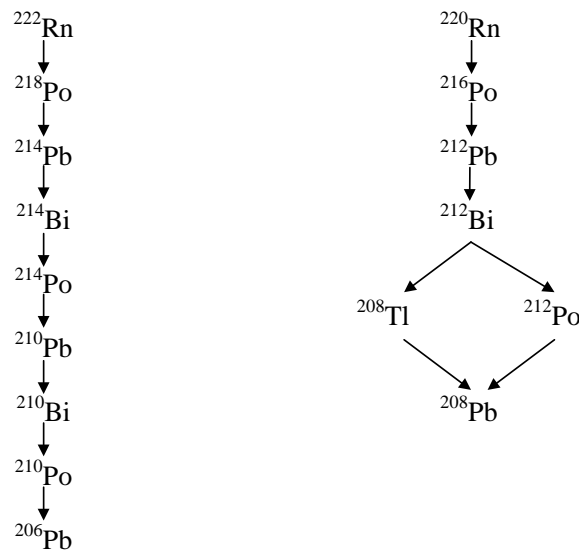
Abstract

Approximately half of the human exposure to radiation is due to indoor airborne short-lived progeny (decay products) of the radon gas (^{222}Rn). To measure the airborne concentrations of radon gas and/or its progeny, Nuclear Track Detectors (NTDs) are usually employed. The NTDs register the alpha particles emitted by radon gas and its progeny in the form of tracks in the NTDs, which will become visible under the optical microscope upon suitable chemical etching of the NTDs. The two most commonly used NTDs are commercially known as CR-39 and LR 115. Calibrations of these NTDs for measurements of concentrations of radon and its progeny can be experimentally performed by exposing the NTDs to known concentrations in exposure chambers. Another approach is to calculate their sensitivities through computer simulations, which enable, among others, better understanding of the involved processes, optimization for the measurements, and determination of calibration coefficients in some circumstances where experimental calibration is not feasible.

Section 1 of this chapter gives a review of existing methods for calculations of calibration coefficients, including Monte Carlo simulations as well as other approaches. Section 2 describes the geometrical model of alpha-particle track formation in NTDs, which will be employed in computer simulations in subsequent sections of this chapter. The two operation modes of the NTD, namely, open mode and the closed mode, are described in sections 2.3 and 2.4, respectively. In Section 2.3, computer codes for calculation of calibration coefficients for NTDs employed in the bare mode are described. The possibility to perform long-term measurements of radon progeny concentrations with bare-mode LR 115 NTDs (by using the "proxy equilibrium factor" which emerges from computer simulations) is presented with more details. Section 2.4 deals with the NTDs employed in the closed mode, i.e., enclosed in the so-called diffusion chambers. Here, the effects of radon progeny deposition onto the inner walls of the diffusion chamber are taken into account. Computer codes are described in details for the calculation of detector sensitivity to alpha particles emitted in the chamber volume and on the chamber wall. Section 3 gives a brief conclusion.

1. Introduction

Approximately half of the human exposure to natural radiation is due to the airborne short-lived progeny of the indoor radon gas (^{222}Rn). The radon gas is originated from the ground and other materials containing its predecessor, ^{226}Ra . In fact, there are different radioisotopes of radon. The most commonly discussed three radioisotopes are ^{222}Rn , ^{220}Rn (thoron) and ^{219}Rn , which are members of the natural radioactive decay series of ^{238}U , ^{232}Th and ^{235}U , respectively. Among these three radioisotopes, ^{222}Rn is the most important due to its the longest half life of 3.825 d and to the larger abundance of ^{238}U in nature. Therefore, when radon is used without specification of a particular radioisotope, it is usually referring to ^{222}Rn . Being an inert noble gas, ^{222}Rn may diffuse from the place of formation and penetrates the boundary surface with the air. Accumulation of ^{222}Rn in a closed space, like the indoor environment of a dwelling, can pose a potential health hazard. The decay schemes of ^{222}Rn and ^{220}Rn are as follows:



Many research papers and books have been devoted to the studies of ^{222}Rn and its short-lived progeny. Various problems related to radon have been investigated such as the measuring techniques, radon penetration properties into houses, dose determination, health risk estimation, etc. On the other hand, radon map on some terrains may help discover underground uranium/thorium ores. It can also serve as a pre-signal for earthquakes or volcano eruptions etc.

Many different methods have been developed for radon measurements. They can be classified according to the duration as grab sampling and long-term measurements. Grab sampling methods, among which the best known is the use of scintillation cells, give information on the ^{222}Rn concentration in a relatively short period of time. (Radon concentration actually refers to the activity concentration of radon with the unit Bq m^{-3} , where the activity refers to the number of disintegrations per unit time with the unit Bq; 1 Bq is equivalent to 1 disintegration on average per unit time.) However, the airborne ^{222}Rn

concentration is subjected to variations so the knowledge in a relatively short period of time might not be representative. In contrast to grab sampling, long-term measurements take much longer time and the average ^{222}Rn concentration during the exposure period can be acquired. The most often used long-term methods are the use of Nuclear Track Detectors (NTDs) and activated charcoal canisters. These two methods do not require any power supply during the operation so that they belong to the group of passive methods. A recent review of properties and applications of NTDs has been given by Nikezic and Yu (2004) and a survey of different operation modes of NTDs for radon measurements was given by Nikolaev and Ilic (1999).

To determine the radon concentration from NTD readings (which is the track density, or the number of tracks per unit area), one needs the knowledge of the detector sensitivity which relates the track density to the total exposure of the detector to radon and its progeny. Experimental determination of this sensitivity, i.e., calibration of these detectors for radon and progeny measurements is carried out by exposing them to known concentrations of radon and/or its progeny in a radon exposure chamber (see e.g., Leung et al. 1994; Yu et al. 2002). Calibration should be carried out with procedures same as those followed in the real life measurements (including procedures for detector processing and readout).

Another approach is to calculate the sensitivities for NTDs through computer simulations, which enable, among others, better understanding of the involved processes, optimization for the measurements and determination of sensitivities under some circumstances where experimental calibration is not feasible. This chapter deals with the mathematical methods and the corresponding computer codes for calculation of calibration factors for radon measurements with NTDs.

1.1. The Principle of NTDs

Heavy charged particles, such as alpha particles, light and heavy ions or fission products, cause extensive ionization when they pass through a medium. For example, an alpha particle ionizes almost all molecules close to its path. This primary ionization triggers a series of new chemical processes that result in the creation of free chemical radicals and other chemical species. Along the path of the alpha particle, a zone enriched with free chemical radicals and other chemical species is then created. This damaged zone is called a latent track and can remain stable for many years in some dielectric materials.

If a piece of material containing latent tracks is exposed to some chemically aggressive solution, chemical reactions would be more intensive along the latent tracks. Aqueous solutions of NaOH or KOH are the most frequently used chemical solutions in this regard. The overall effect is that the chemical solution etches the surface of the detector material, but with a faster rate in the damaged region. In this way, a track (or sometimes called pit) of the particle is formed, which may be seen under an optical microscope. This procedure is called detector etching or track visualization, and the effect itself is called the track effect.

The track effect exists in many materials. It is particularly pronounced in materials with long molecules, e.g., cellulose nitrates or different polycarbonates, and such materials are the most convenient ones for manufacturing as well as for applications. The effect is also seen in some amorphous materials like glasses. A comprehensive survey on the materials that show the track effect is given by Fleischer et al. (1975). More recently, the track effect has also

been found in some metals, intermetallic compounds and superconducting oxides (Fleischer 2002).

One of the most commonly used NTDs is the CR-39 detector, which was based on polyallyldiglycol carbonate and was discovered by Cartwright et al. (1978). Another most commonly used nuclear track material is cellulose nitrate, with the most well-known NTD being sold under the commercial name LR 115. Other kinds of detectors are also in use, such as the Makrofol detector which is based on polycarbonate. Some natural materials that show the track effect, such as apatite, mica, olivine, etc., are used for fission or fossil track studies.

Although the track effect is relatively well known, and the techniques involved are rather simple and straightforward, there is no unique theory that explains the process of track formation. The basic physical processes after the initial charged particle loses its energy are the ionization and excitation of molecules of the material. This first physical phase in which the initial particle delivers its energy to the atoms surrounding its path is very short in time; stopping of the particle occurs within a time in the order of ps. The free electrons created in these primary interactions will slow down through a series of ionizations and excitations, and will create more and more free electrons. Some of these may go further away from the initial particle path creating the so-called delta rays (δ -rays). A large number of free electrons and damaged molecules are created close to the particle track.

In the second physiochemical phase, new chemical species are created by interactions of the damaged molecules. During etching, the interactions of these new chemical species with the etching solution (or called etchant) are stronger than those with the undamaged detector material. However, it is not known which chemical species are formed after the particle passage through the material, and the nature of damage is also not entirely known. Different theories have been developed in order to understand these processes (Fleischer et al. 1965; Seitz and Koehler 1956; Chadderton and Montagu-Pollock 1963; Barillon et al. 1999).

1.2. Bulk and Track Etch Rates, and Geometry of the Track Growth

From the early beginning of track science, the formal description of track growth had attracted significant attention. Formation of a track is determined by the simultaneous action of two etching rates, V_b and V_t , as introduced by Fleischer et al. (1975). The bulk etch rate V_b is the etching rate of the undamaged detector surface, while the track etch rate V_t is the etching rate along the latent track. Both rates are usually expressed in the unit $\mu\text{m}\cdot\text{h}^{-1}$. Several methods were developed and applied to determine V_b , which were based on, e.g., the track diameter of fission fragments, the mass difference before and after etching (Kocsis et al. 1997), direct measurements by using surface profilometry (Nikezic and Janicijevic, 2002; Yip et al., 2003a) or atomic force microscopy (AFM) (Yasuda et al. 1998; Ho et al. 2002), absorption of x-ray fluorescence photons (Yip et al., 2003b), infrared absorption (Ng et al. 2004) and gray level determination (Yu and Ng 2004), etc. It has been shown that V_b depends on the detector material as well as temperature, molarity and intensity of stirring of the etchant (see Nikezic and Yu 2004 for a review). Pre-etching storage, age and irradiation by x-ray, gamma-ray or UV radiation of the detector also affect V_b . On the other hand, much fewer results are available for V_t in different detector materials, which is likely due to the much more difficult measurements of V_t when compared to V_b . Although several theories of track

formation have been developed, the mechanisms behind the chemical etching are not fully understood.

Several models have been proposed, which enable calculations of the track parameters and plotting of the track profile and opening contour. Some of the existing models were recently discussed and compared by Nikezic and Yu (2004) and Nikezic et al. (2006). The major axes of track openings in the CR-39 detector were calculated from different models for alpha particles with various incident angles and energies. Good agreement was obtained among different models with the existing set of experimental data.

1.3. Methods for Determining NTD Sensitivity to Radon and Its Progeny

There are two groups of methods to calculate the NTD sensitivity to radon and its progeny. The first group is based on analytical derivation of a formula for the sensitivity, while the second group is based on Monte Carlo simulations.

Analytical calculations of the detection probability have been performed for open-mode as well as for closed-mode NTDs, which involve integration over the space in front of NTDs.

The open mode involves the use of a bare NTD, where the NTD is simply immersed for a fixed time in the atmosphere for which the radon concentration is to be measured. The closed mode involves the use of a closed NTD, where an NTD is placed inside a chamber covered with some permeable material such as a filter paper. In the case of open detectors, an upper limit on the detector sensitivity can be calculated based on the Cherry formula (Cherry 1964):

$$N = \frac{RA}{4}$$

where N is the number of alpha particles striking the detector per second, R is the alpha-particle range in air (in cm) and A is the airborne concentration of alpha-particle emitting radionuclides ($\text{Bq}\cdot\text{m}^{-3}$). There are three alpha-particle emitters in the ^{222}Rn chain with alpha-particle energies of 5.49 MeV (^{222}Rn), 6 MeV (^{218}Po) and 7.69 MeV (^{214}Po). The corresponding ranges in air are 4.09, 4.67 and 6.78 cm, respectively. According to previous data and assuming that the airborne concentrations of radon and its progeny are all $1 \text{ Bq}\cdot\text{m}^{-3}$, the maximum partial sensitivities are

$$\rho_{^{222}\text{Rn}} = 0.088 \text{ (track/cm}^2\text{)/(Bq}\cdot\text{d/m}^3\text{)} = 0.01 \text{ (track/m}^2\text{)/(Bq}\cdot\text{s/m}^3\text{)}$$

$$\rho_{^{218}\text{Po}} = 0.1 \text{ (track/cm}^2\text{)/(Bq}\cdot\text{d/m}^3\text{)} = 0.011 \text{ (track/m}^2\text{)/(Bq}\cdot\text{s/m}^3\text{)}$$

$$\rho_{^{214}\text{Po}} = 0.146 \text{ (track/cm}^2\text{)/(Bq}\cdot\text{d/m}^3\text{)} = 0.017 \text{ (track/m}^2\text{)/(Bq}\cdot\text{s/m}^3\text{)}$$

The total sensitivity is the sum of partial sensitivities so the maximum sensitivity (assuming equilibrium between radon and its progeny, i.e., assuming they have the same activity concentrations) is

$$s_{total} = 0.334 \text{ (track/cm}^2\text{)/(Bq}\cdot\text{d/m}^3\text{)} = 0.038 \text{ (track/m}^2\text{)/(Bq}\cdot\text{s/m}^3\text{)}$$

This is the maximum sensitivity which can be obtained with NTDs. Here, the plateau (i.e., the deposited radon progeny on the NTD surfaces) has not been taken into account. The observed sensitivity (or the actual number of tracks) after etching will be smaller because etching will not transform all latent tracks into visible tracks and some alpha particles will have incident angles smaller than the critical angle. In the case of closed-mode NTDs, the chamber walls change the irradiation geometry and disturb the previous considerations.

Fleischer and Mogro-Compero (1978) employed the equation

$$N = \iint A(r, \theta) \sin 2\theta \, dr \, d\theta$$

where N is again the track density per unit exposure time and A is the airborne concentration of alpha-particle emitter. The integration has to be performed over the effective volume from which the emitted alpha particles can be detected by the detector. The activity A can be taken as constant (although some researchers have shown that the radon progeny concentration decreases close to a surface due to deposition), and a formula similar to the Cherry formula was obtained as

$$N = \text{constant} \times A/4$$

When compared to the Cherry formula, the difference is the introduction of the “effective volume” which is defined as the volume in front of the detector from which the emitted alpha particles have non-zero detection probabilities. Alpha particles emitted beyond the effective volume cannot be detected. This concept will be used in Monte Carlo simulations, which will be described below. The shape and size of the effective volume depend on the alpha-particle energy, the etching condition, readout procedures and the size and shape of the detector. Since three groups of alpha particles are emitted in ^{222}Rn chain, three different effective volumes have to be determined for the same detector and etching conditions. Some researchers used formulas which were variants of the above equations. In most cases, the integration limit was set according to the critical angle.

Another group of calculations is based on the Monte Carlo method, in which simulations of alpha particle histories are performed (described in the next section). For a brief survey of Monte Carlo calculations of NTD sensitivity, the readers are referred to our previous review paper (Nikezic and Yu 2004). It is remarked that the Monte Carlo method enables easier incorporation of an appropriate track formation model (including etching conditions and readout procedures) than in analytical approaches.

1.4. Monte Carlo Method

The Monte Carlo method is based on computer simulation of processes (not only physical processes) that are statistical in nature by using random numbers. For example, the emission of an alpha particle is a statistical process. One cannot be sure when a nucleus will decay and emit an alpha particle. Instead, we can only talk about the probability of it undergoing decay in a particular time interval. When the decay takes place, the direction in which the alpha particle is emitted is also random. There is a chain of randomness in the emission,

propagation and detection of alpha particles, and the overall process is conveniently followed by Monte Carlo simulations.

The Monte Carlo method has been described in many books and only a short description is given here, which is necessary to understand the following text. The method is based on standard random numbers which are uniformly distributed numbers greater than or equal to 0 and less than 1. It is possible to produce random numbers by some physical devices, e.g., the number of pulses obtained from a detector in one second is a random number, but they are not uniformly distributed and they do not fall between 0 and 1. Such production of random numbers can be rather slow and it is not very convenient for computer simulations.

Random number generators are used in computer simulations, which are small programs which generate random numbers as outputs by using some suitable algorithms. Many algorithms have been described in the literature. In these algorithms, usually a number RN_i is obtained on some manipulation of a previously obtained number RN_{i-1} . Such numbers are not really random because it is possible to predict the next one if the algorithm is known, and this is why they are called pseudorandom numbers. To produce the series of random numbers, one needs to provide the first one which is called the seed. The same series of numbers is produced for the same seed. In Fortran 90 and 95, depending on the user's need, there are several methods for invoking the random number generator. One of them is the intrinsic function `CALL RANDOM_NUMBER(rn)`. This command will produce one random number which will be assigned to the variable "rn" (the name can be chosen by the user). For example, the following section of the program

```
DO I=1,10
CALL RANDOM_NUMBER(x)
WRITE(*,10)x
END DO
10 FORMAT(' ',F8.6)
```

will produce the following output

```
.000022
.085032
.601353
.891611
.967956
```

Each new run of the program will produce the same series of random numbers. This is convenient for the control and debugging of the program. However, if a user wishes to have a different series of random numbers in each new run of the program, the intrinsic Fortran 90 function `CALL RANDOM_SEED()` should be used.

Standard random numbers obtained from the previous function are in the range between 0 and 1. These numbers are used to obtain random numbers distributed in other ranges by simple multiplications. For example, the uniform point on the x axis between points A and B ($x_A < x_B$) can be obtained as $x_{\text{random}} = x_A + (x_B - x_A)RN$ where x_A and x_B are the coordinates of points A and B, and RN is random number between 0 and 1. The same approach can be applied to choose random points between points C and D on the y axis using a similar

formula $y_{\text{random}} = y_C + (y_D - y_C)RN$. In this way, a random point in the rectangle ABCD in plane xOy can be chosen. Such a procedure is usually called sampling. In the above case, it is a sampling of random points within the rectangle. This simple procedure can be used to estimate the value of an integral of a function $f(x)$ within the interval from A to B, assuming that we can calculate values of this function for all given values of the independent variable x . A short computing plan can be as follows:

1. Determine the maximal value f_{max} of the function $f(x)$ in a given interval.
2. Sample one random point in the rectangle given by the coordinates $x_{\text{random}} = x_A + (x_B - x_A)RN_1$ and $y_{\text{random}} = f_{\text{max}} \cdot RN_2$.
3. Examine the condition $y_{\text{random}} < f(x_{\text{random}})$. If yes, increase "counter N_{below} " by 1. This counter counts the number of points below the curve $f(x)$.
4. Repeat steps 2 and 3 for N times.

The integral is then evaluated through
$$\int_{x_A}^{x_B} f(x)dx = \frac{N_{\text{below}}}{N} (x_B - x_A) f_{\text{max}}.$$

The accuracy of calculation depends on the number of points N sampled within the rectangle. This example can be used as a model for sampling of points on some arbitrary surface on a plane.

Sampling of random points within a volume can be performed in a similar way by introducing the third coordinate z . For example, for sampling of a random and uniform point R within a parallelepiped shown in Fig.1, which is limited by the points A, B and C with coordinates $(x_A, y_A, 0)$, $(x_B, y_B, 0)$ and (x_A, y_A, z_C) , the following set of equations can be used:

$$\begin{aligned} x_r &= x_A + (x_B - x_A) \cdot RN_1 \\ y_r &= y_A + (y_B - y_A) \cdot RN_2 \\ z_r &= z_C \cdot RN_3 \end{aligned}$$

where RN_i , $i = 1, 2$ and 3 are three random numbers.

To perform a Monte Carlo simulation of particle detection, we need to sample random directions in the space. Two angles, namely the polar angle φ and the azimuth angle θ , determine a direction in space. The angle φ ranges between 0 and 2π so the random angle φ_R is found as

$$\varphi_R = 2\pi RN_1 \quad (1)$$

The random angle θ_R (with a range from 0 to π) is sampled in a somewhat different way as

$$\cos \theta_R = 2RN_2 - 1 \quad (2)$$

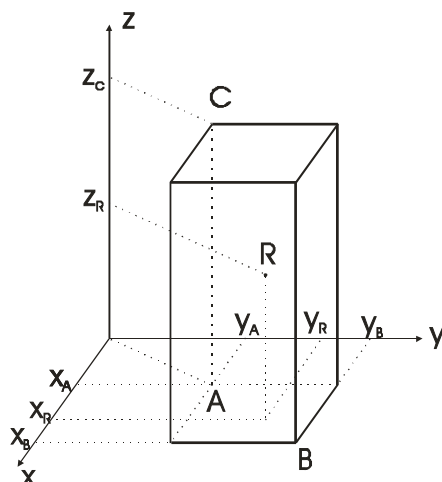


Figure 1. Sampling of a random point R in a parallelepiped.

2. Simulation of Radon Measurements with NTDs

As described in section 1.3, NTDs are used in the open and closed modes for radon measurements. This section is devoted to discussion of radon measurements with bare detectors (i.e., in the open mode). Alpha particles emitted by airborne radon and its short lived progeny bombard the detector and leave latent tracks in the detector material. In this way, the bare detector registers signals from both radon and its short-lived progeny.

Measurements for the radon gas concentration with the bare detector are not reliable because the equilibrium factor between the radon gas and its progeny can be variable from one place to another, so the number of tracks contributed by the radon progeny depends on the equilibrium factor. The equilibrium factor F is defined as $F = 0.105F_1 + 0.515F_2 + 0.380F_3$, where F_1 , F_2 and F_3 are the ratios of the activity concentrations of ^{218}Po , ^{214}Pb and $^{214}\text{Bi(Po)}$ to that of ^{222}Rn , and quantify the equilibrium between the radon gas and its progeny.

It is impossible to distinguish between the tracks produced by radon gas and those by its progeny. Similarly, the bare detector cannot be simply used for radon progeny measurements. It is necessary to determine the radon gas concentration separately and then to determine the contribution from the radon to the number of tracks on the detector. One can then obtain the number of tracks due to radon progeny by subtracting these tracks from the total number on the detector. Here, the main problem is the determination of the number of tracks contributed from radon only. To solve this problem, we need simulations where one assumes that only radon is present in air.

2.1. Requirements for and Outputs from Simulations

What do we get from simulations?

The outputs from the simulations are the detection efficiencies ε , i.e., the probability for detection. The detection efficiency may be determined as a ratio between the number of registered particles in the simulations to the total number of simulations. However, this number is not enough because the sensitivity s for radon measurements with NTDs is defined as the number of tracks per unit surface area of the detector per unit exposure to radon. A unit exposure is the exposure of the detector in an atmosphere with a radon concentration of 1 Bq/m³ for 1 s. In this way, the unit for the calibration coefficient k will be [m⁻²]/[Bqm⁻³s] = [m].

To obtain the sensitivity from the detection efficiency ε , one needs to assume that the activity of radon (or another alpha emitter) is $C_0 = 1 \text{ Bqm}^{-3}$. The total number of emitted alpha particles for the irradiation time $t = 1 \text{ s}$ is then given by $V \times C_0 \times t$ where V is volume of the space in front of detector from which the emitted alpha particles can reach the detector. It is clear that the space is limited by the ranges of the alpha particles in air. However, if the alpha particles come from distances that are too close to the end of their ranges, they strike the detector with too small energies which will become insufficient to generate etchable tracks. Furthermore, some alpha particles have incident angles below the critical angle for track formation and, again, they will not be registered. Therefore, it is necessary to define the effective volume where the initial points of alpha particles should be sampled. The effective volume is the space in front of the detector from which the emitted alpha particles have non-zero probabilities for registration at the detector. Determinations of the effective volume for alpha particles with a given incident energy and for a known removed layer of the NTD form the first step in the computer simulation.

What do we need to perform the simulations?

To perform the computer simulations, we need the following information:

- (a) energy-distance curve for alpha particles in air,
- (b) energy-range curve for alpha particles in the detector,
- (c) the removed layer h of the detector during the etching time t ($h = V_b t$),
- (d) criterion for visibility of the etched alpha-particle tracks,
- (e) V function, i.e., the ratio between the track etch rate V_t and the bulk etch rate V_b (i.e., $V = V_t/V_b$),
- (f) model for growth of tracks in the detector.

(a) Energy-distance curve for alpha particles in air

To obtain the energy-distance curve in air, one should use the data about the stopping power S of alpha particles in air. There are several computer codes that can be used to produce tables with stopping power as a function of the alpha-particle energy. In the present chapter, we will refer to the well-known and widely used program called SRIM (Stopping and Range of Ions in Matter). The program is freely downloadable from <http://www.srim.org/#SRIM> and the version to which we are referring in this chapter is the one published in 2003, which will be hereafter referred to as SRIM2003. As default, SRIM2003 uses an air density of 0.00125 gcm⁻³ and this should be corrected for the room

temperature to $0.001208 \text{ gcm}^{-3}$. A fraction of the output table from SRIM2003 is given in Table 1.

Table 1. Stopping power of alpha particles in air obtained from SRIM2003 (partial output).

Ion = Helium [2] , Mass = 4.003 amu
Target Density=1.2080E-03 g/cm3= 4.9131E+19 atoms/cm3

===== Target Composition =====

Atom Name	Atomic Numb	Atomic Percent	Mass Percent
O	8	023.20	025.07
N	7	075.50	071.42
Ar	18	001.30	003.51

Stopping Units = MeV / cm

Ion Energy	dE/dx (Elec)	dE/dx (Nuclear)	Projected Range	Longitudinal Straggling	Lateral Straggling
10.00 keV	3.775E-01	7.291E-02	180.80 um	75.22 μm	65.70 μm
100.00 keV	1.194E-00	1.571E-02	1.17 mm	175.72 μm	207.82 μm
200.00 keV	1.654E-00	9.182E-03	1.84 mm	197.84 μm	251.48 μm
500.00 keV	2.291E-00	4.376E-03	3.31 mm	227.32 μm	304.34 μm
1.00 MeV	2.262E-00	2.454E-03	5.44 mm	269.70 μm	348.78 μm
2.00 MeV	1.652E-00	1.359E-03	10.62 mm	393.07 μm	428.94 μm
3.00 MeV	1.290E-00	9.579E-04	17.52 mm	644.97 μm	531.58 μm
4.00 MeV	1.071E-00	7.458E-04	26.05 mm	904.23 μm	662.66 μm
5.00 MeV	9.210E-01	6.137E-04	36.14 mm	1.37 mm	821.60 μm
6.00 MeV	8.104E-01	5.230E-04	47.72 mm	1.82 mm	1.01 mm
7.00 MeV	7.248E-01	4.566E-04	60.77 mm	2.26 mm	1.22 mm
8.00 MeV	6.563E-01	4.059E-04	75.26 mm	3.08 mm	1.45 mm
9.00 MeV	6.064E-01	3.658E-04	91.10 mm	3.83 mm	1.71 mm
10.00 MeV	5.596E-01	3.332E-04	108.25 mm	4.56 mm	1.98 mm

There are two different stopping powers, which are due to nuclear and electronic interactions, which should be summed up to obtain the total energy loss of alpha particles in air. The stopping power of alpha particles in air is given as

$$-\frac{dE}{dx} = f(E)$$

where $f(E)$ is a function obtained by fitting the data obtained from SRIM2003. To fit the previous data, the following formula (with 15 constants) was used:

$$f(E) = \sum_{i=1}^5 A_i E^{B_i} e^{C_i E}$$

where the best fit parameters are found as:

$$\begin{aligned} A(1) &= 3.3548 \times 10^{-4}; & A(2) &= 2.7682 \times 10^{-9}; & A(3) &= 5.4642; & A(4) &= 10.1733; & A(5) &= 0.7761 \\ B(1) &= 5.4271; & B(2) &= -3.3294; & B(3) &= 0.5999; & B(4) &= 2.5507; & B(5) &= 1.6561 \\ C(1) &= -0.5427; & C(2) &= 2.3181; & C(3) &= -1.1553; & C(4) &= -4.9027; & C(5) &= -0.5454 \end{aligned}$$

The function with these best-fit parameters is shown in Fig. 2.

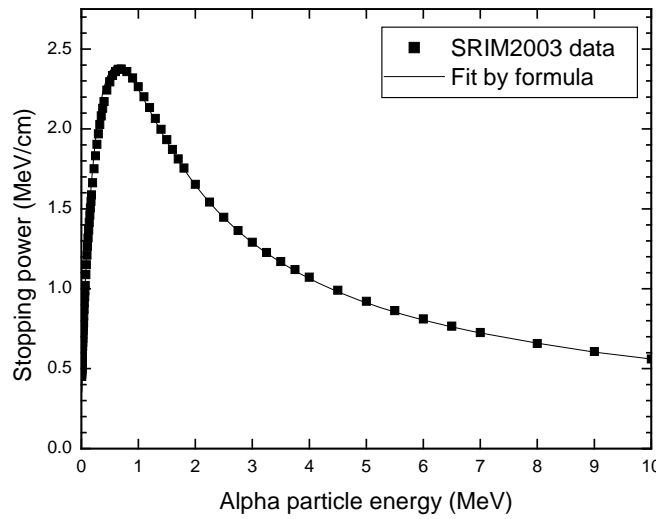


Figure 2. Stopping power (in MeV/cm) of alpha particles in air at room temperature calculated using the SRIM2003 code.

The energy E_L of the alpha particles after traveling a distance L in air can be determined by solving the previous equation, i.e.,

$$L = \int_0^L dx = \int_{E_L}^{E_0} f(E)$$

where E_0 is the initial energy of alpha particles. In this equation, the known quantity is L while the unknown quantity is the lower bound of the integration E_L . To solve this equation, one should use iterations. Such a procedure is rather time consuming because the integral has to be evaluated numerically many times for each given L . The alternative approach is to systematically change E_L with small steps (which is 0.001 MeV in the program shown below), calculate L for each E_L and store results in a energy-distance table. The program called ENERGY_DISTANCE.F90 performs this operation.

```
PROGRAM DIST_ENERGY
!CALCULATES ENERGY OF ALPHA PARTICLES AFTER SOME DISTANCE IN AIR
!BASED ON STOPPING POWER CURVE SP(E) OBTAINED BY SRIM2003
REAL(4),DIMENSION (5):: A, B, C
OPEN (100,FILE='OUTPUT_A10000.DAT')
EALPHA=10 !ALPHA ENERGY IN MeV
!FITTING CONSTANTS FOR AIR DENSITY 0.001208 g/cm3
A(1)=3.3548e-4; A(2)=2.7682e-9;A(3)=5.4642;A(4)=10.1733;A(5)=0.7761
B(1)=5.4271; B(2)=-3.3294; B(3)=0.5999;B(4)=2.5507; B(5)=1.6561
C(1)=-0.5427; C(2)=2.3181; C(3)=-1.1553; C(4)=-4.9027; C(5)=-0.5454
E=EALPHA
DO
PRINT *, E
CALL DINT1(EALPHA,E,DISTANCE)
SP=FUNCT(E)
WRITE(100,*)DISTANCE,E
E=E-0.001
IF(E<=0.)EXIT
END DO
CONTAINS
SUBROUTINE DINT1(G,D,VRINT)
!NUMERICAL INTEGRATION
COMMON /ZONA1/DOETC,VO
SUM=0.
H=(G-D)/500.
DVR=1./FUNCT(D)
GVR=1./FUNCT(G)
ET=D
DO I=1,499
ET=ET+H
FJA=1./FUNCT(ET)
SUM=SUM+FJA
END DO
SUMA=DVR+GVR+2.*SUM
SUMA=H*SUMA/2.
VRINT=SUMA
RETURN
END SUBROUTINE DINT1
FUNCTION FUNCT(X)
SUMA=0.
DO I1=1,5
SUMA=SUMA+A(I1)*X**B(I1)*EXP(C(I1)*X)
END DO
FUNCT=SUMA
END FUNCTION FUNCT
END PROGRAM DIST_ENERGY
```

The output from this program has two columns, the first one giving the distance in air and the second giving the energy of alpha particles after passing through the distance given in the first column (taking the initial alpha energy as 10 MeV). The results are graphically shown in Fig. 3.

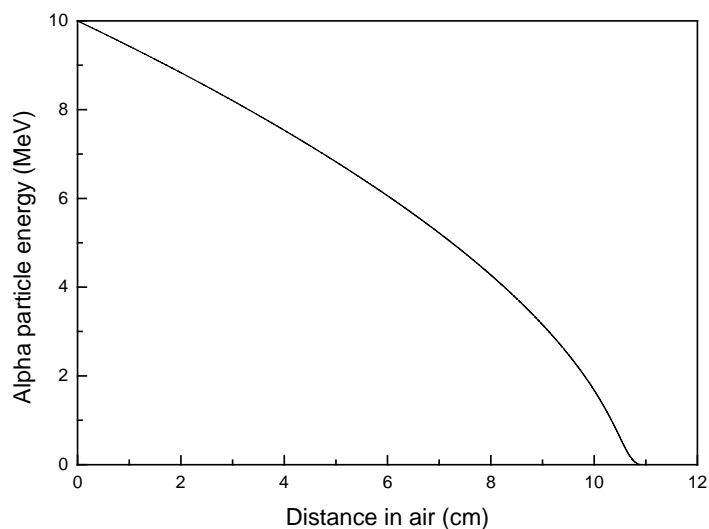


Figure 3. Energy-distance curve for alpha particles in air.

In the course of simulation, the known quantity is L and the energy of an alpha particle is obtained by a linear interpolation between the two closest values of energies. Since the step is relatively small, the error of such an approach is smaller than 1 keV. In this way, the simulation is significantly accelerated.

(b) Energy-range curve for alpha particles in the detector

The most frequently used detector for radon measurements are CR-39 and LR 115, and the following text will be devoted to these two detectors only. It is necessary to first determine the range of alpha particles in these detector materials. For this purpose, the SRIM2003 code will be used again.

The CR-39 detector is based on polyallyldiglycol carbonate with the chemical formula $C_{12}H_{18}O_7$ and a density $\rho = 1.32 \text{ gcm}^{-3}$. On the other hand, the LR 115 is based on cellulose nitrate with a chemical formula $C_6H_8O_9N_2$ and a density of $\rho = 1.4 \text{ gcm}^{-3}$. The energy-range curves for these two detectors are shown in Fig. 4.

As shown in Fig. 4, the ranges in CR-39 and LR 115 are rather similar, with those for LR 115 being slightly larger. This is not very surprising because the chemical formulas and densities are similar. However, their response to the alpha particles, i.e., the track formation does not only depend on the stopping power and ranges, but is mostly determined by the nature and chemical reactivity of the chemical radicals and other chemical species created in the track core after the passage of an ionizing heavy particle. The numerical data for Fig. 4 are stored in the files RANG_LR_SRIM.DAT and RANG_CR_SRIM.DAT in the form of the

two-column tables. In the simulations, the range of an alpha particle with a known energy in a detector is found by linear interpolation between two the closest values in the relevant table.

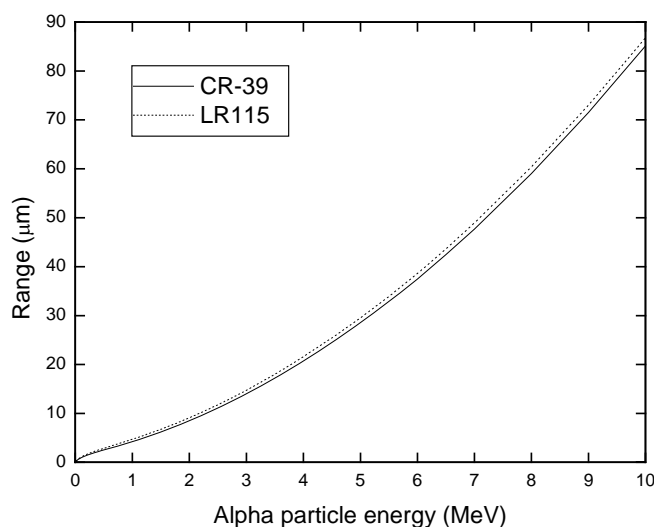


Figure 4. Ranges (in μm) of alpha particles in CR-39 (solid line) and LR 115 (dotted line) detectors as a function of alpha-particle energy, which are calculated using SRIM2003.

(c) *Removed layer h of the detector during the etching time t ($h = V_b t$)*

The removed layer h is determined as $h = V_b t$, where V_b is the bulk etch rate and t is the etching time. Both these quantities should be provided in the file INPUT.DAT as the third and fourth variables. The first variable in the file INPUT.DAT is either the character C (for CR-39) or L (for LR 115). If some other character is provided, the program will stop. The second parameter in INPUT.DAT is the alpha particle energy (in MeV).

(d) *Criterion for visibility of etched alpha-particle tracks*

The alpha-particle tracks are usually counted under the optical microscope, although other techniques (semi- or fully automatic) are also known. One should introduce some realistic visibility criteria in the computer simulations, e.g., objects with too small dimensions are not counted because they cannot be seen under the microscope. The visibility criterion is the fifth variable in the file INPUT.DAT.

(e) *V function, i.e., the ratio between the track etch rate V_t and the bulk etch rate V_b*

Several functions are programmed and the user can choose any one by inserting the number of the corresponding function as the sixth parameter in file INPUT.DAT. The V function is calculated in the subroutine VT.F90. All subsequent calculations will be performed only with the chosen function.

For the CR-39 detector, the following functions are available:

(1) Durrani and Bull (1987): $V = 1 + (11.45e^{-0.339R'} + 4e^{-0.044R'}) (1 - e^{-0.58R'})$

(2) Brun et al. (1999): $V = 1 + e^{-a_1R'+a_4} - e^{-a_2R'+a_3} + e^{a_3} - e^{a_4}$
with the constants $a_1 = 0.1$, $a_2 = 1$, $a_3 = 1.27$ and $a_4 = 1$.

(3) Yu et al. (2005a): This is similar to function (2), i.e., $V = 1 + e^{-a_1R'+a_4} - e^{-a_2R'+a_3}$
but with constants $a_1 = 0.068$, $a_2 = 0.6513$, $a_3 = a_4 = 1.1784$.

(4) Yu et al. (2005b): the same as function (3) but with constants
 $a_1 = 0.06082$, $a_2 = 0.8055$, $a_3 = a_4 = 1.119$.

For the LR 115 detector, the following functions are available:

(1) Durrani and Green (1984): $V = 1 + (a_1e^{-a_2R'} + a_3e^{-a_4})(1 - e^{-R'})$
with constants $a_1 = 100$, $a_2 = 0.446$, $a_3 = 5$, $a_4 = 0.107$.

(2) Yip et al. (2006): The same form as function (1), but with constants
 $a_1 = 2.14$, $a_2 = 0.12$, $a_3 = 2.7$, $a_4 = 0.135$.

(3) Leung et al. (2006a): The same form as function (1), but with constants
 $a_1 = 14.50$, $a_2 = 0.5$, $a_3 = 3.9$, $a_4 = 0.066$.

(3) Leung et al. (2006b): The same form as function (1), but with constants
 $a_1 = 14.23$; $a_2 = 0.48$; $a_3 = 5.9$ and $a_4 = 0.077$

(f) Model for growth of tracks in the detector

The model of track growth is the most important issue here. The model of track formation proposed by Nikezic and Yu (2003) is implemented in the subroutine DETNIK.F90. That is almost the same program as TRACK_TEST.F90 described by Nikezic and Yu (2006) and thus will not be described here.

As the output from DETNIK.F90, the track parameters are given, including the major and minor axes of the track opening, the depth of the track and the variable entitled INDICATOR. This variable is equal to -1 if the track does not pass the visibility criterion, i.e., if the track dimensions are smaller than predetermined values (chosen by the user) or if the track has not been developed at all. INDICATOR is equal to +1 if the track is visible according to the preset criteria. The subroutine DETNIK.F90 outputs other information related to the track, such as the track profile, opening contour, 3-D coordinates of the track (the user can create a 3-D image with a suitable software), but such outputs are disabled here since these are not relevant to radon measurements.

2.2. Program QUEST.F90

The program QUEST calculates the effective volume in front of the detector and outputs in the file EV.DAT. The effective volume is given in the form of a table, in which the first column gives the angle (in degrees) with respect to the normal to the detector surface, the second and the third columns give the minimal and maximal distances in air from which the emitted alpha particles can be detected. If an alpha particle is emitted outside the given range, it cannot be detected. The fourth and the fifth columns are the minimal and maximal energies of the alpha particle that can be detected; in other words, these constitute the energy window. The following is a sample segment from file EV.DAT:

```
10 1.9000 3.9090 1.7061 4.2994
11 1.9000 3.9090 1.7061 4.2994
```

Here, the first number “10” means 10° with respect to the normal (i.e. 80° with respect to the surface). The next two numbers, 1.9000 and 3.9090 (cm), represent the distance range from which the emitted alpha particle with the given energy can be detected. In other words, if the alpha particle is emitted closer than 1.9 cm or beyond 3.9 cm, it will not be registered. The minimal and maximal distances (variables RMIN and RMAX in the program QUEST) depend on the initial alpha particle energy, the removed layer of the NTD during etching and the visibility criteria. The numbers (in MeV) in the fourth and fifth columns (1.7061 and 4.2994) constitute the energy window. Alpha particles should strike the detector with energies within this energy window in order to be detected. For example, the energy should be between 1.7061 and 4.2994 MeV for the incident angle of 10° (with respect to the normal to the detector). In contrast to the minimal and maximal distances, the energy window does not depend on the initial alpha-particle energy or the material in front of the detector. The energy window only depends on the etching condition and the visibility criteria.

The program QUEST.F90 works in the following way. Firstly, it reads the input parameters from the file INPUT.DAT. Then it reads the data from the file OUTPUT_A10000.DAT where the energy-distance curve of alpha particles in air is given in the form of a table with the energy step of 1 keV. The calculations start with normal incidence (incident angle = 0° with respect to the normal to the detector surface) and the distance in air that is equal to the range of alpha particles in air for the initial energy given in INPUT.DAT. Since the alpha particle emitted from the distance that is equal to the range will strike the detector with zero energy, the distance in air is reduced by 0.1 cm and the impact energy is calculated using the energy-distance curve. The program DETNIK.F90 is then invoked, which returns INDICATOR = -1 if the track is invisible or not formed. If the track is not formed, the distance is further reduced for 0.1 cm and the process is repeated until detection is obtained at a particular distance or when the distance comes to zero. When the detection occurs, the corresponding distance RMAX and energy EMIN are stored in the computer memory. The incident angle is then increased by 1° and the distance is reset to the alpha-particle range in air and the whole procedure is repeated. When examinations for all 90 incident angles have been completed, the determination of RMIN and EMAX start again from normal incidence, but here the distance starts from zero (i.e., the particle emitted on the detector surface with the incident energy given in INPUT.DAT) and increases with small

steps of 0.1. The procedure is completed when all incident angles from 0° to 90° and all distances from zero to the range are examined.

The described procedure might look too time consuming. However, once it is run and completed, there is no need to run it again until some of the input parameters (e.g., the etching condition, visibility criteria or V function) are changed. The file EV.DAT can also be stored under different names and used later. When the effective volume and the effective energy windows have been calculated for a given set of input parameters, one can perform calculations for the detector irradiated under different conditions (but etched and read in the same way).

To execute the program QUEST.F90, the subroutines DETNIK8B.F90, DINT3.F90, LINEAR_INTERPOLATION.F90 and VT.F90 should be copied and INSERTed in the same directory (working space) and compiled together.

The routine VT.F90 is a FUNCTION type of subprogram and calculates the value of V for a given residual range for a chosen detector and a chosen V function. This subroutine is given below:

```
DOUBLE PRECISION FUNCTION VT(Y)
DOUBLE PRECISION Y,PI
DOUBLE PRECISION THETAG,VB
CHARACTER *1,DETECTOR
COMMON DETECTOR,VB,PI,THETAG,VISIBILITY,NFUNCTION
!Y IS RESUDUAL RANGE of alpha particle in detector
IF(DETECTOR=='C') THEN !BLOCK FOR CR DETECTOR
IF(NFUNCTION==1)THEN
VT= 1.+(11.45*EXP(-0.339*Y)+4.*EXP(-0.044*Y))*(1.-EXP(-0.58*Y))
END IF
IF(NFUNCTION==2)THEN
A1F=0.1
A2F=1.
A3F=1.27
A4F=1.
VT=1.+EXP(-A1F*Y+A4F)-EXP(-A2F*Y+A3F)+EXP(A3F)-EXP(A4F)
RETURN
END IF
IF(NFUNCTION==3)THEN
vt=1.+exp(-0.068*y+1.1784)-exp(-0.6513*y+1.1784)
END IF
IF(NFUNCTION==4) THEN
A1FO=0.06082
A2FO=0.8055
B1FO=1.119
VT=1.+DEXP(DBLE(-A1FO*Y+B1FO))-DEXP(DBLE(-A2FO*Y+B1FO))
RETURN
END IF
END IF !END OF THE BLOCK FOR CR-39 DETECTOR

IF(DETECTOR=='L')THEN !BLOCK FOR LR115 DETECTOR
```

```

IF(NFUNCTION==1)THEN
VT=1.+(100.*EXP(-0.446*Y)+5.*EXP(-0.107*Y))*(1.-EXP(-Y))
RETURN
END IF

IF(NFUNCTION==2)THEN
A1C=2.14
A2C=0.12
A3C=2.7
A4C=0.135
VT=1.+(A1C*EXP(-A2C*Y)+A3C*EXP(-A4C*Y))*(1.-EXP(-Y))
RETURN
END IF

IF(NFUNCTION==3) THEN
A1=14.50
A2=0.5
A3=3.9
A4=0.066
VT=1.+(A1*EXP(-A2*Y)+A3*EXP(-A4*Y))*(1.-EXP(-Y))
RETURN
END IF

IF(NFUNCTION==4) THEN
A1P=14.23
A2P=0.48
A3P=5.9
A4P=0.077
VT=1.+(A1P*EXP(-A2P*Y)+A3P*EXP(-A4P*Y))*(1.-EXP(-Y))
RETURN
END IF
END IF !END OF BLOCK FOR LR115 DETECTOR
END FUNCTION VT

```

The subroutine LINEAR_INTERPOLATION.F90 is used by the subroutine DETNIK.F90 and performs a linear interpolation between four points in order to find the cross section between two lines. One line is drawn between points in the track wall and the second line represents the post-etched surface. By finding their intersection, the points where the track starts or where it ends can be determined. The subroutine LINEAR_INTERPOLATION.F90 is given below:

```

SUBROUTINE LINEAR_INTERPOLATION(REM,THETA,X1A,Y1A,X2A,Y2A,XP,YP)
DOUBLE PRECISION REM,X1A,Y1A,X2A,Y2A,XP,YP,THETA
BROJILAC=(X1A*Y2A-X2A*Y1A)/(X1A-X2A)- REM/COS(THETA)
BIMANILAC=-TAN(THETA)-(Y1A-Y2A)/(X1A-X2A)
XP=BROJILAC/BIMANILAC
YP=-TAN(THETA)*XP+REM/COS(THETA)
END SUBROUTINE LINEAR_INTERPOLATION

```

Finally, the subroutine DINT3.F90 calculates numerically the following integral

$$\int_0^R \frac{1}{V(R-x)} dx$$

where R is the particle range in the detector material and x is the distance from the entry point of the particle into the detector to some point along the particle trajectory. This subroutine is called several times from DETNIK.F90 with different integration limits.

2.3. Simulation of Radon Measurements with a Bare NTD

In this mode of radon measurements, the NTD is simply immersed in air and the alpha particles emitted by the airborne (radon + progeny) and (thoron + progeny) can generate latent tracks in the NTD. No other important alpha-particle emitters can be found in air under normal circumstances, but cosmic radiation can create some background tracks.

Monte Carlo simulations of radon measurements with bare NTDs can be performed in two somewhat different ways. The first one involves the concept of the effective volume from which the emission points are only sampled. The second one samples starting points of alpha particles in the volume in front of the detector within the range of alpha particles in air. The calculations presented here have made use of the effective volume, and we will compare the two methods at a later stage.

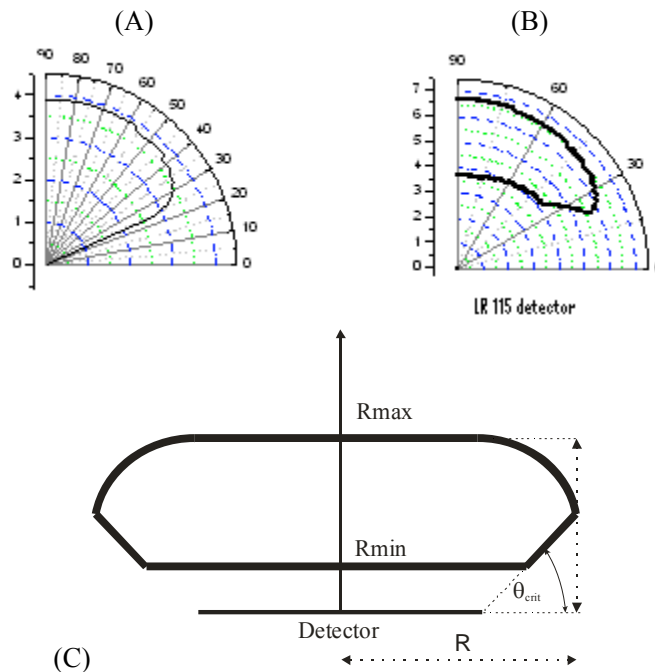


Figure 5. The cross-section of the effective volume for a point-like detector in polar diagrams: (A) for the CR-39 NTD and 6 MeV alpha particles; (B) for the LR 115 NTD, 7.69 MeV alpha particle and 9 μm of removed layer. (C) Extension from the point-like detector to a real detector.

The program QEUST.F90 determines the effective volume for a point like detector. Examples of the effective volumes for the CR-39 and LR 115 NTDs are given in Fig. 5 in the polar diagram. Here the intersections between the effective volumes and the vertical planes are shown. Rotation of the curves in Fig. 5 around the vertical axis will generate the 3-D effective volume for the point-like detector. Simulations and measurements with a point-like detector will give zero results because of the zero probability to target a singular point. In reality, the detectors are not point like and have some finite dimensions which are usually a few cm. Extrapolation of the effective volume determined for a point-like detector to a detector with finite dimensions is not a trivial task and it is performed in the following way. For a real detector, the effective volume is the sum of effective volumes of all points on the detector. The effective volume directly above the detector (which is taken to be circular for the discussion here) has a cylindrical shape with the base equal to the circular detector. The portion of the effective volume that is not directly above the detector follows the shape of the effective volume for the point-like detector. The real effective volume is then obtained by rotation of the region shown in Fig.5 (C) around the z-axis.

2.3.1. Calculation of Partial Sensitivities: OPEN_DETECTOR.F90

The program OPEN_DETECTOR.F90 performs simulations of (radon + progeny) measurements with NTDs. The program first reads input data from the file INPUT.DAT as for the case when the effective volume was determined. The program then reads the file EV.DAT where the effective volume is given. The simulations consist of several steps:

(a) Sampling of random points within the effective volume. Since the effective volume has an irregular shape (see Fig. 5(C)), the rejection technique is applied here, which is described as follows. Points are sampled randomly in a cylinder with the radius R and height R_{\max} , which encompasses the whole effective volume, and the number of such sampled points is N . Only those points which fall within the effective volume are taken as starting points of the alpha particles, and the number of such points is N_s . The effective volume V_{eff} (in cm^3) is then calculated as $V_{\text{eff}} = (N_s/N)\pi R^2 R_{\max}$.

(b) Sampling of the random direction through Eqs. (1) and (2) in the section on the Monte Carlo Method.

(c) Decision on whether the alpha particle is emitted towards the detector. If not, the program returns to step (a). If yes, the distance between the emission point and the entry point in the detector is calculated. If this distance is larger than the particle range in air, again, the program returns to step (a). If the particle strikes the detector, the distance from the emission point to the entry point is compared with the data given in EV.DAT for a given incident angle. If this distance is within the detectable range, the number of scoring N_{sc} is increased by 1; if not, the control returns to step (a).

(d) When the number of scoring achieves a pre-determined number, the program leaves the simulation loop and calculates the efficiency as $\varepsilon = N_{\text{sc}}/N_s$, i.e., the ratio between the number of registered and emitted alpha particles. The sensitivity is then calculated as:

$$\rho_i = \frac{\varepsilon_i V_i}{\pi r^2} \quad i = 1, 2, 3$$

where r is the detector radius, ρ_i are the partial sensitivities; $i = 1, 2, 3$ refer to ^{222}Rn , ^{218}Po and ^{214}Po , respectively. Here the activity A of a radon progeny species is taken to be $A = 1 \text{ Bqm}^{-3}$ and the irradiation time t taken as $t = 1 \text{ s}$. The product $V \times A \times t$ is then the number of particles emitted in the effective volume per 1 s. Multiplying it with the detection efficiency gives the number of tracks per unit exposure. Dividing this with the surface area of the detector, πr^2 , one obtains the sensitivity (in track/m² per Bqsm⁻³ or just in m). In this way, we can obtain the sensitivity to one particular alpha-particle emitter, which is called the partial sensitivity. This quantity is not directly measurable because it is almost impossible to obtain only one type of alpha-particle emitter in the air.

The program OPEN_DETECTOR.F90 should be run three times for three different alpha-particle emitters in the ^{222}Rn chain. A different effective volume has to be used each time. The total sensitivity s for radon measurements, which is the ultimate goal of these calculations, is contributed by all the partial sensitivities.

The average radon concentration C during the exposure time is calculated by $C = k\rho$, where k is the calibration coefficient [Bqsm⁻³/(track/m²)] and ρ is the track density per unit irradiation time (track/m²s). The total sensitivity s is the reciprocal of the calibration coefficient, i.e., $s = 1/k$. For the LR 115 NTD, one can write $s = \rho_0 + \rho_1 + \rho_3$ where ρ_0 , ρ_1 and ρ_3 are the partial sensitivities to ^{222}Rn , ^{218}Po and ^{214}Po , respectively. For the CR-39 detector, the above equation is not valid since this detector does not have an upper energy limit. This detector will thus even register those alpha particles emitted by radon progeny atoms that are plated out on the detector surface. Since the amount of plateout radon progeny is unknown, the bare CR-39 NTD is not recommended for radon measurements.

2.3.2. Some Simulation Results

The partial sensitivities have been calculated for the CR-39 and LR 115 NTDs and are presented in Figs. 6 and 7, respectively, with the removed layer as a parameter. The partial sensitivity for the CR-39 detector slightly increases with the removed layer and achieves saturation. In other words, all existing latent tracks are developed after some time, and further etching only enlarges the tracks but does not increase their number. On the other hand, the partial sensitivity for the CR-39 detector increases significantly with the energy of emitted alpha particles.

Different patterns are observed for the partial sensitivities for the LR 115 NTD. Again, this is due to the existence of upper and lower energy limits in this detector. The most important finding here is the equality of partial sensitivities for different energies if the removed layer is smaller than $\sim 7.5 \mu\text{m}$. For larger removed layers, the sensitivity increases slightly with the alpha-particle energy. For removed layers smaller than $\sim 7.5 \mu\text{m}$, one can write $\rho_0 = \rho_1 = \rho_3$ and thus $s = \rho_0 + \rho_1 + \rho_3 = 3\rho_0$. The total number of tracks ρ on the LR 115 NTD is then equal to $\rho = \rho_0(C_0 + C_1 + C_3)t$ where C_0 , C_1 and C_3 are the airborne concentrations of ^{222}Rn , ^{218}Po and $^{214}\text{Bi(Po)}$ (in Bq/m³) and t is the exposure time. If C_0 is known (e.g. from a separate measurement), we can obtain the sum $(C_1 + C_3)$ given as

$$C_1 + C_3 = \frac{\rho}{\rho_0 t} - C_0$$

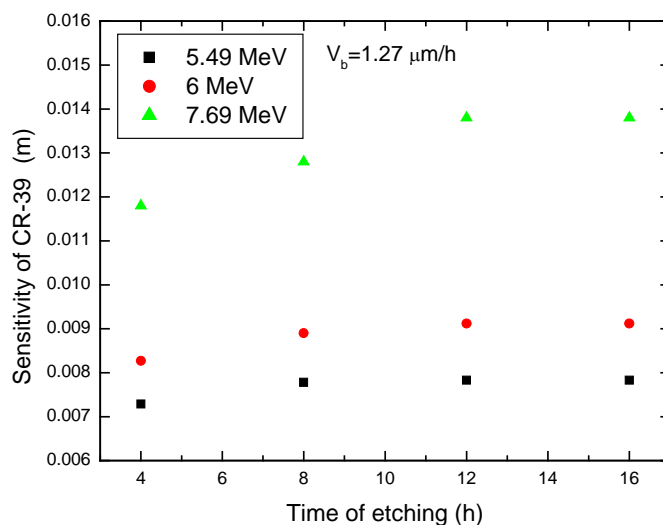


Figure 6. Sensitivities of the CR-39 detector to three alpha-particle energies emitted in the ^{222}Rn chain, which are calculated with a bulk etch rate of $V_b = 1.27 \mu\text{m/h}$.

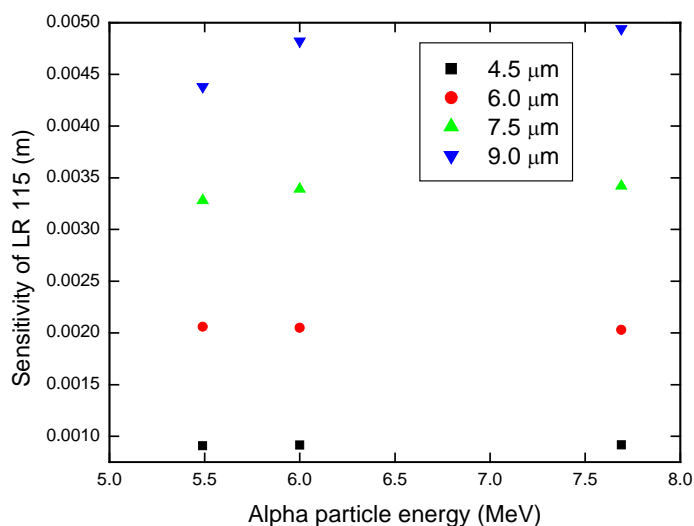


Figure 7. Sensitivities of the LR 115 detector to three alpha-particle energies in the ^{222}Rn chain, with the removed layer as a parameter, which are calculated with the V function (1) (see section 2.1(e)).

Dividing with C_0 , we can have

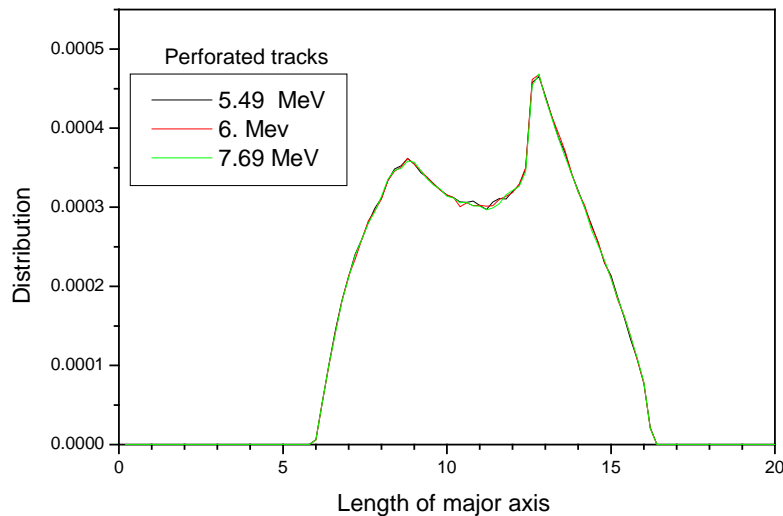
$$\frac{C_1}{C_0} + \frac{C_3}{C_0} = \frac{\rho}{\rho_0 t C_0} - 1 = F_1 + F_3 = F_p$$

Here, F_1 and F_3 are the ratios of the airborne activity concentrations of ^{218}Po and $^{214}\text{Bi}(\text{Po})$ to that of ^{222}Rn . Their sum is called the “proxy equilibrium factor” or F_p (Nikezic at al. 2004). It has been shown that F_p is related to the equilibrium factor F between radon gas and its progeny in a relatively good manner (Yu et al. 2005c). Based on these findings, a method for long-term measurement of the equilibrium factor has been proposed recently (Nikezic at al. 2004, Yu et al. 2005c).

2.3.3. Calculation without the Effective Volume: OPEN_DETECTOR_1.F90

As mentioned earlier, radon measurements with NTDs can be simulated without involving the concept of the effective volume. However, it is necessary to limit the space from which the starting points of the alpha particles are sampled. It is natural to employ the alpha-particle ranges in air, which will avoid complications about the effective volume. However, one should invoke the subroutine DETNIK.F90 for every alpha particle that hits the detector, and such calculations are rather time consuming. For example, a Pentium computer with a 1.6 GHz CPU and 504 MB of RAM memory needs about 2 s to perform the calculations for one registered particle. This means about 1800 registered particles will be simulated in 1 h. This is rather slow since 10^4 registrations are needed to get a relative uncertainty of 1 %.

In order to compare between the two approaches, the program OPEN_DETECTOR.F90 is modified in the section where the decision about detection is made. The modified version of the program is called OPEN_DETECTOR_1.F90 (note the extension `_1` here). In OPEN_DETECTOR.F90, the incident alpha-particle energy on the detector is compared with the upper and lower energy limits given in EV.DAT (this is equivalent to a comparison of distances). In the second version, OPEN_DETECTOR_1.F90, decision will be made after invoking the subroutine DETNIK.F90 which returns the track parameters and the INDICATOR (which is equal to +1 if the track is visible or -1 if not).



(a)

Figure 8. continued on next page.

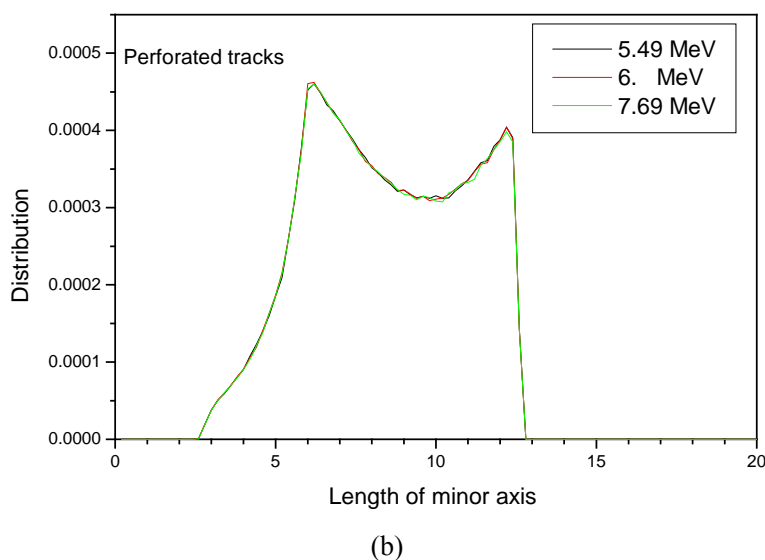


Figure 8. Distribution of the lengths of (a) major axis and (b) minor axis for perforated tracks in LR 115 (Yu et al. 2005c).

It might have been expected that the two programs give exactly the same results, but this is not the case because the step used in the determination of the effective volume is finite. The angle was changed for 1° and the distance for 1 mm. For example, the comparison for the LR 115 NTD shows that a difference between the two programs, which is, however, less than 4 %.

Although the calculations with OPEN_DETECTOR_1.90 are much slower, this program gives some more information, such as the size distribution of the major and minor axes of the track opening, for a given set of etching and readout conditions. One such example is shown in Fig. 8. It is interesting to observe from Fig. 8 that the curves for three alpha-particle energies in the radon chain overlap almost completely for the entire ranges of the lengths for both major and minor axes. From this result, we see that the partial sensitivities for the LR 115 detector to ^{222}Rn , ^{218}Po and ^{214}Po are the same. The bimodal distributions shown in Fig. 8 can be explained through analyses of angular and energy distributions of alpha particles incident on the detector and are related to the track formation model.

2.4. Simulation of Radon Measurements with NTD in Diffusion Chamber

Radon gas measurements are usually performed with NTDs in the closed mode. In this method, an NTD is placed inside a diffusion chamber closed at the top with a permeable filter. In this way, only the ^{222}Rn gas diffuses into the chamber (that is why this device is called the diffusion chamber) while the radon progeny are stopped on the filter. In addition, the filter stops dust and water vapor from entering the chamber, thus making radon measurements less dependent on environmental conditions. A schematic sketch of a conical diffusion chamber with a detector placed on its inner bottom is given in Fig. 9. Here, the height of the diffusion chamber is H , its base and top radii are R_1 and R_2 , respectively, and the radius of the detector is R_{det} .

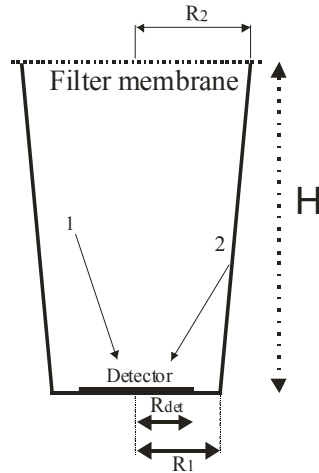


Figure 9. A conical diffusion chamber (with a height H , base radius R_1 and top radius R_2) with an NTD (with radius R_{det}) placed on the inner bottom.

The radon atoms inside the chamber can decay and create new progeny, which may further decay whilst in the air volume of the chamber or after their deposition on the chamber wall. There are three types of alpha-particle emitters in air (^{222}Rn , non-deposited fraction of ^{218}Po and ^{214}Po) denoted by “1” in Fig. 9, and those on the chamber wall (deposited fraction of ^{218}Po and ^{214}Po) denoted by “2” in Fig. 9, and emitters deposited on the detector itself (plateout ^{218}Po and ^{214}Po). Only the first two sources are important for the LR 115 NTD (due to the upper energy threshold for registration of alpha particles for this NTD as discussed above), while all three sources are important for the CR-39 NTD.

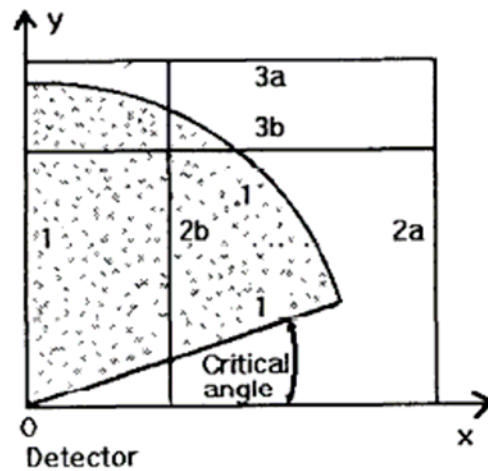


Figure 10. Intersection of an arbitrary effective volume (shaded area) for a point-like detector at point 0, and the vertical and horizontal walls of the chamber (Nikezic et al. 1996).

Here the irradiation geometry is significantly changed in comparison to case for the bare detector. The chamber wall can intersect with the effective volume of the detector, which leads to a reduction in the partial sensitivities. The possible cases are shown in Fig. 10.

Fig. 10 shows an arbitrary effective volume (shaded area enclosed by curve 1) for a point-like detector at point 0. The two possible positions for the vertical chamber walls are denoted by the lines 2a and 2b. In the case 2a, the chamber wall does not cut the effective volume and alpha particles emitted from the wall will not be detected. In contrast, the vertical wall cuts the effective volume in the case 2b. The horizontal wall (membrane filter) can also be outside of the effective volume (case 3a) or inside it (case 3b). All these cases should be treated separately when the alpha particles emitted from the wall (2a or 2b) are considered. If the vertical wall cuts the effective volume, the partial sensitivity for detection of radon progeny in the air volume is reduced because the wall prevents detection of some particles that would have been detected by the bare detector.

The total sensitivity s of the detector is the sum of the partial sensitivities that are multiplied by factors representing the partitioning of radon progeny between air and the chamber wall:

$$s = \rho_0 + f_1\rho_{1a} + f_3\rho_{3s} + (1 - f_1)\rho_{1w} + (1 - f_3)\rho_{3w} + p_1N_1 + p_3N_3 \quad (3)$$

where ρ_{ia} are the partial sensitivities for ^{222}Rn ($i = 0$), ^{218}Po ($i = 1$) and ^{214}Po ($i = 3$) from air, and ρ_{iw} ($i = 1,3$) from the wall, p_i ($i = 1,3$) are the probabilities for plateout detection, N_i ($i = 1,3$) are the numbers of progeny atoms which decay on the detector surface (with a unit area) per unit time and per unit radon activity in air, and f_i ($i = 1,3$) are the airborne fractions (the fractions that decay in the air volume in the diffusion chamber). As discussed before, the probabilities p_i are equal to zero for the LR 115 NTD.

All the variables in Eq. (3) can be calculated by computer programs which are similar to the previously described program OPEN_DETECTOR.F90. Three additional programs have been prepared: CHAMBER.F90, WALL.F90 and PLATE.F90. The difference among these three programs is in the section where the starting points of alpha particles are sampled. Other elements of the programs are essentially the same.

2.4.1. Program CHAMBER.F90

This program calculates the partial sensitivities to radon progeny inside the chamber volume. The program is written for a general conical chamber where the base radius R_1 is smaller than the top radius R_2 , i.e., $R_1 < R_2$. The program can also be used for a cylindrical chamber with the input $R_1 = R_2$.

The program starts with reading the data from INPUT_CHAMBER.DAT, where the following variables are given: DETECTOR (can be C for CR-39 or L for LR 115), EALFA (alpha particle energy), NREGOG (number of registered alpha particles), R1C, R2C, HA (base and top radii, and height of the diffusion chamber), RDET (detector radius) and NFUNCTION (the identification number of V function in the subroutine VT.F90). The energy-distance curve of alpha particles in air is then read from the file OUTPUT_A10000.DAT, and the range of alpha particles with the given energy is determined. The next step is to read the effective volume from the file EV.DAT. The user should be cautious in using the effective volume which corresponds to the data in the file INPUT_CHAMBER.DAT. Here, the points are first chosen within the effective volume, and the points outside the diffusion chamber are then rejected. Other elements of the program are the same as those in OPEN_DETECTOR.F90.

2.4.2. Program WALL.F90

This program calculates the sensitivities of the LR 115 and CR-39 NTDs to the alpha-particle emitters deposited on inner wall of the diffusion chamber. The deposition of the radon progeny is assumed to be uniform although some newer findings claim that this is not fully correct (Palacios et al. 2005, Nikezic and Stevanovic 2005).

The source of alpha particles is obtained as the intersection between the effective volume and the chamber wall, which is called the effective surface. In this way, we can distinguish the following cases: (i) the only source is the vertical wall, which is denoted as the lines 2b-3a in Fig. 10; (ii) the only source is the filter at the opposite side of the detector, denoted as the lines 3b-2a, (ii) the source comprises the vertical wall and the filter, denoted as the lines 3b-2b, and (iv) the effective volume is completely within the chamber, in which case there will not be any calculations and the program stops. All these cases are separately treated in the program.

It is important to first determine the points between which the effective surface is situated. For example, the conical part of the wall cuts the effective volume at points A and B in Fig. 11. The effective surface is then obtained as the revolution of the segment AB around the vertical axis passing through the center of the detector (in this case, the center of the detector overlaps with the center of the base of the diffusion chamber). Similarly, the horizontal part of the wall intersects with the effective volume at points C and D in Fig. 11.

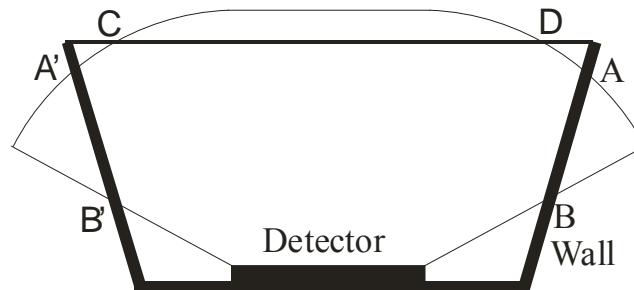


Figure 11. Intersection between the walls of the diffusion chamber and the effective volume. The effective surface comprises the segments between points A and B and between C and D.

It is important to know the surface area (in cm^2) of the effective surface. The area of the conical part S_{co} of the effective surface can be obtained through an analytical formula, while the horizontal part S_{ci} of the effective surface is part of a circle, so the total effective surface area S_t is given by $S_t = S_{co} + S_{ci}$. The initial points of alpha particles are sampled only between A and B, and/or between C and D. The sensitivity is then obtained as follows. For simplicity, we consider the concentration of an alpha-particle emitter inside the diffusion chamber as $C_0 = 1 \text{ Bqm}^{-3}$. Based on the volume and surface area, we can determine the surface activity C_s (in Bqm^{-2}). The product of C_s and the detection efficiency ε obtained from Monte Carlo simulations gives the total number of tracks on the detector per unit exposure of 1 s. By dividing this with the detector area, one obtains the sensitivity expressed in track/m^2 per Bqsm^{-3} , which is our task. Other elements of the program are essentially the same as those in CHAMBER.F90 and OPEN_DETECTOR.F90.

2.4.3. Program PLATE.F90

The program calculates the sensitivity of the detector to the progeny deposited on the detector itself. The geometry considered here is much simpler in comparison to the previous cases. The initial points of alpha particles are chosen just on the detector surface. Some alpha particles may be attached to the aerosols which are deposited on the surface. However, the diameters of aerosol particles are in general much smaller than the ranges of alpha particles so this complication can be neglected.

This program is not needed for the LR 115 NTD because the detector does not register alpha particles from the plateout radon progeny. As a first approximation, one can assume that the registration efficiency of the CR-39 detector is 50 %, meaning that only half of the alpha particles are emitted towards the detector. Of course, this is not exactly the case because some particles will strike the detector with incident angles below the critical angle for track formation. Some tracks from alpha particles under oblique incidence will be developed with a delay. With prolonged etching, more and more tracks will be revealed. This explains the trend of the relationship between the detection efficiency and the removed layer as shown in Fig. 12.

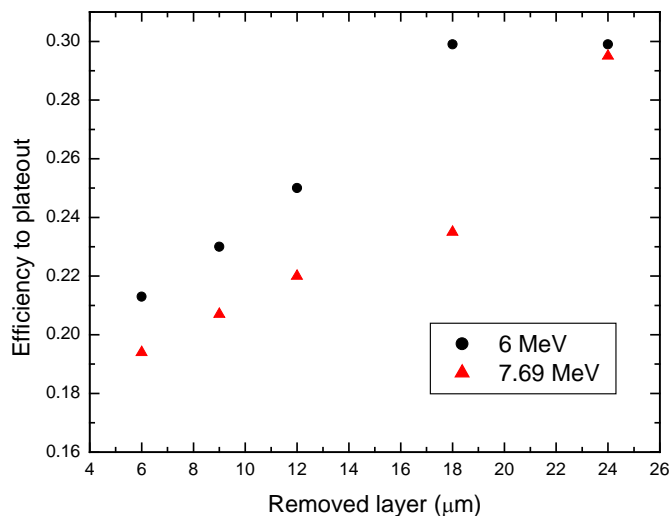


Figure 12. The detection efficiency of the CR-39 NTD to alpha particles emitted on the detector surface (i.e., from the plateout radon progeny) as a function of the removed layer during etching.

To calculate the contribution from the plateout radon progeny to the total sensitivity, one can multiply the efficiency shown in Fig. 12 with the number of alpha particles emitted per unit detector surface per unit time (i.e., N_i in Eq. (3) in section 2.4), considering an airborne radon concentration of 1 Bqm^{-3} .

3. Conclusion

In the present chapter, computer programs for calculating the NTD sensitivity to radon and its progeny have been described. The NTDs operated in the open (bare) mode and in the closed

mode (in the diffusion chamber) have been treated separately because the irradiation geometries are not the same. The programs can be used for CR-39 and LR 115 NTDs, but extension to other types of NTDs are also possible if relevant information (such as the V functions) is provided. The programs also enable optimization of the diffusion chamber, e.g., determination of its optimal dimensions and shape.

References

- Barillon, R., Fromm, M., Chambaudet, A., Katz, R., Stoquert, J.P., Pape, A. 1999. Bond scission cross sections for alpha-particles in cellulose nitrate (LR115). *Radiat. Meas.* **31**, 71-75.
- Brun, C., Fromm, M., Jouffroy, M., Meyer, P., Groetz, J.E., Abel, F., Chambaudet, A., Dorschel, B., Hermsdorf, D., Bretschneider, R., Kadner, K., Kuhne, H., 1999. Intercomparative study of the detection characteristics of the CR-39 SSNTD for light ions: Present status of the Besancon-Dresden approaches. *Radiat. Meas.* **31**, 89-98.
- Cartwright, B.G., Shirk, E.K., Price, P.B. 1978. Nuclear-track-recording polymer of unique sensitivity and resolution. *Nucl. Instr. Methods* **153**, 457-460.
- Chadderton, L.T., Montagu-Pollock, H.M., 1963. Fission fragment damage to crystal lattice. Heat sensitive crystals. *Proc. Roy. Soc.* **A274**, 239-252.
- Cherry, R.D., 1964. In *The Natural Radiation Environment*, J.A.S Adams (Ed.) (Univ. of Chicago Press) (1964) 407-424.
- Durrani, S.A., Bull, R.K., 1987. *Solid State Nuclear Track Detection. Principles, Methods and Applications*. Pergamon Press.
- Durrani, S.A., Green, P.F., 1984. The effect of etching conditions on the response of LR 115. *Nucl. Tracks* **8**, 21-24.
- Fleischer, R.L. 2002. Ion Tracks. Chapter 14 in "Intermetallic Compounds: Vol. 3, Principles and Practice". Ed. J.H. Westbrook and R.L. Fleischer. John Wiley & Sons, Chichester, U.K., p. 263-273.
- Fleischer, R.L., Mogro-Compero, A., 1978. Mapping of integrated radon emanation for detection of long-distance migration of gases within earth - techniques and principles. *J. Geophys. Res.* **83** (NB7), 3539- 3549.
- Fleischer, R.L., Price, P.B., Walker, R.M. 1965, The ion explosion spike mechanisms for formation of charged particle tracks in solids. *J. Appl. Phys.* **36**, 3645-3652.
- Fleischer, R.L., Price, P.B., Walker, R.M. 1975. *Nuclear Tracks in Solids*. University of California Press, Berkley.
- Ho, J.P.Y., Yip, C.W.Y., Koo, V.S.Y., Nikezic, D., Yu, K.N. 2002. Measurement of bulk etch rate of LR115 detector with atomic force microscopy. *Radiation Measurements*, **35**, 571-573.
- Kocsis, Z.S., Dwivedi, K.K., Brandt, R. 1997. Studies on the track formation mechanism of the heavy ions in CR-39. *Radiat. Meas.* **28**, 177-80.
- Leung, J.K.C., Jia, D., Tso, M.Y.W., 1994. A Fully Automated Radon Exposure Chamber. *Nucl. Instrum. Meth. Phys. Res. A*; **350**, 566-571.
- Leung, S.Y.Y., Nikezic, D., Leung, J.K.C., Yu, K.N., 2006a. Derivation of V function for LR 115 SSNTD from its sensitivity to ^{220}Rn in a diffusion chamber. *Applied Radiation and Isotopes*, in press.

- Leung, S.Y.Y., Nikezic, D., Yu, K.N., 2006b. Derivation of V function for LR 115 SSNTD from its partial sensitivity to ^{222}Rn and its short-lived progeny. *Journal of Environmental Radioactivity*, in press.
- Nikezic, D., Baixeras, C., Kostic, D., 1996. Sensitivity determination and optimisation of a cylindrical diffusion chamber for radon measurements with a CR39 detector. *Nuclear Instruments and Methods in Physics Research A* **373**, 290-298.
- Nikezic, D., Janicijevic, A., 2002. Bulk etching rate of LR 115 detector. *Appl. Radiat. Isotop.* **57**, 275-278.
- Nikezic, D., Kostic, D., Yip, C.W.Y., Yu, K.N., 2006. Comparison among Different Models of Track Growth and Experimental Data. *Radiation Measurements*, **41**, 253-256.
- Nikezic, D., Ng, F.M.F., Yu, K.N., 2004. Theoretical basis for long-term measurements of equilibrium factor using LR 115 detector. *Appl. Radiat. Isot.* **61**, 1431-1435.
- Nikezic, D., Stevanovic, N., 2005. Radon progeny behavior in diffusion chamber. *Nuclear Instruments and Methods in Physics Research B* **239**, 399-406.
- Nikezic, D., Yu, K.N., 2003. Three-dimensional analytical determination of the track parameters. Over-etched tracks, *Radiation Measurements*, **37**, 39-45.
- Nikezic, D., Yu, K.N., 2004. *Formation and Growth of Tracks in Nuclear Track Materials. Materials Science and Engineering R* **46**, 51-123.
- Nikezic, D., Yu, K.N., 2006, Computer program TRACK_TEST for calculating parameters and plotting profiles for etch pits in nuclear track materials, *Computer Physics Communications*, **174**, 160-165.
- Nikolaev, V.A., Ilic, R., 1999. Etched track radiometers in radon measurements: a review *Radiat. Meas.*; **30**, 1-13.
- Ng, F.M.F., Yip, C.W.Y., Ho, J.P.Y., Nikezic, D., Yu, K.N. 2004. Non-destructive Measurement of Active Layer Thickness of LR 115 SSNTD. *Radiation Measurements*, **38**, 1-3.
- Palacios, D., Sajo-Bohus, L., Greaves, E.D., 2005. Radon progeny distributions inside a diffusion chamber and their contributions to track density in SSNT detectors. *Radiation Measurements*, **40**, 657-661.
- Seitz, F., Koehler, J.S., 1956. Displacement of atoms during irradiation. *Solid State Phys.* **2**, 305-448.
- Yasuda, N., Yamamoto, M., Miyahara, N., Ishigure, N., Kanai, T., Ogura, K., 1998. Measurement of bulk etch rate of CR-39 with atomic force microscopy. *Nucl. Instrum. Methods B* **142**, 111-116.
- Yip, C.W.Y., Ho, J.P.Y., Koo, V.S.Y., Nikezic, D., Yu, K.N., 2003a. Effects of stirring on the bulk etch rate of LR 115 detector. *Radiation Measurements*, **37**, 197-200.
- Yip, C.W.Y., Ho, J.P.Y., Nikezic, D., Yu, K.N., 2003b. A fast method to measure the thickness of removed layer from etching of LR-115 detector based on EDXRF. *Radiation Measurements*, **36**, 161-164.
- Yip, C.W.Y., Nikezic, D., Ho, J.P.Y., Yu, K.N., 2006, Chemical Etching Characteristics for Cellulose Nitrate. *Materials Chemistry and Physics*, **95**, 307-312.
- Yu, K.N., Koo, V.S.Y., Guan, Z.J., 2002. A simple and versatile $^{222}\text{Rn}/^{220}\text{Rn}$ exposure chamber. *Nuclear Instruments and Methods in Physics Research Journal A*, **481**, 749-755.
- Yu, K.N., Ng, F.M.F. 2004. Fast and non-destructive determination of active-layer thickness of LR 115 SSNTD using a color commercial document scanner. *Nuclear Instruments and Methods in Physics Research Journal (Section B)*, **226**, 365-368.

- Yu, K.N., Ho, J.P.Y., Nikezic, D., Yip, C.W.Y., 2005a. Determination of the V function for CR-39 by atomic force microscope. In *Recent advances in multidisciplinary applied physics*. Ed. Antonio Mendez-Vilas. Elsevier, Amsterdam, p. 29-34.
- Yu, K.N., Ng, F.M.F., Nikezic, D., 2005b. Measuring depths of sub-micron tracks in a CR-39 detector from replicas using atomic force microscopy. *Radiat. Meas.* **40**, 380-383.
- Yu, K.N., Nikezic, D., Ng, F.M.F., Leung, J.K.C., 2005c. Long-term measurements of radon progeny concentrations with solid state nuclear track detectors. *Radiat. Meas.* **40**, 560-568.